

The influence of spacetime curvature on quantum emission in optical analogues to gravity

Maxime J Jacquet^{1,*} and Friedrich König^{2,†}

¹Faculty of Physics, University of Vienna, Boltzmannngasse 5, Vienna A-1090, Austria.

²School of Physics and Astronomy, SUPA, University of St. Andrews,
North Haugh, St. Andrews, KY16 9SS, United Kingdom

(Dated: 14th December 2024)

Quantum fluctuations on curved spacetimes cause the emission of pairs of particles from the quantum vacuum, as in the Hawking effect from black holes. We use an optical analogue to gravity (see [1]) to investigate the influence of the curvature on quantum emission. Due to dispersion, the spacetime curvature varies with frequency here. We analytically calculate for all frequencies the particle flux, correlations and entanglement. We find that horizons increase the flux with a characteristic spectral shape. The photon number correlations transition from multi- to two-mode, with close to maximal entanglement. The quantum state is a diagnostic for the mode conversion in laboratory tests of general relativity.

In a curved spacetime, quantum fluctuations lead to the spontaneous emission of particles. Famously, if the curved spacetime contains an event horizon, it is predicted to emit pairs of particles via the Hawking effect [2, 3]. However, the (static) black hole event horizon is not the only ‘regime of spacetime curvature’ that leads to particle emission. Analogue spacetimes are effective wave media that allow for table-top experiments on configurable curved spacetimes [4]. In addition to static black holes [5–11], it is also possible to create *e.g.* (static) white hole event horizons [5, 7, 10, 12–16], rotating geometries analogous to Kerr black holes [17, 18], expanding universes [19, 20] or even (static) two-horizon interactions [21, 22]. For these systems featuring a static horizon, the traditional benchmark to demonstrate analogue gravity physics has been the observation of the classical effect of frequency shifting of waves as they scatter at the horizon. Importantly, the scattering of waves that could not be associated with a horizon has also been observed in ‘fluid’ systems [12, 14, 23–29]. In this context, the question of the influence of the spacetime curvature on quantum emission in analogues to gravity arises: *e.g.* what differentiates emission at the horizon (the Hawking effect) from horizonless emission? Here, we use a simple, optical system to find out what are the signatures of emission in different spacetimes.

From quantum field theory in curved spacetimes, we know that the mechanism at the heart of horizon and horizonless emission is the same [3, 4, 30, 31]. In this light, correlated pairs from horizons are considered an unmistakable signature of the Hawking effect [32–34], and have thus been extensively studied for fluid systems, in which their entanglement in various dispersive regimes has been investigated [35–41]. However, these studies have not contrasted horizon and horizonless emission, and neither has this been done in optics.

In optics, the curvature of the background on which light propagates is achieved by changing the speed of light with light itself [5, 7, 10, 13, 42, 43]: a short and intense laser pulse locally raises the refractive index n of a medium by the Kerr effect, such that other light under the pulse is slowed by this increase in n . Even a small increase in the index will create an event horizon [44]: there will always be certain modes which get slowed below the pulse speed and are captured by its front,

in analogy with the kinematics of waves around a black-hole event horizon [4, 45]. But, in fact, this is not the sole kinematic scenario (*i.e.*, the trajectory of waves) that is realised at the front. Hence this optical system allows us to contrast the quantum emission in different kinematic scenarios.

In this letter, we use a simple, moving step-like refractive index front (RIF) propagating in a dispersive, optical medium as an example analogue gravity system. The RIF is a powerful theoretical platform because it allows to consider a single point of interest in the index profile of a dispersive system and is thus analytically accessible. Because of dispersion in the system, the kinematic scenario continuously changes with frequency, and scenarios yielding horizon-like and horizonless interactions are realised simultaneously. We present all the possible kinematic scenarios for modes at the RIF and thus explain how the interplay between the step height (the magnitude in the index change) and the dispersion of the system gives rise to distinct regimes of spacetime curvature. We then use an analytical method developed in [46][1] to describe the scattering of modes at the RIF and calculate the spontaneous emission in each regime of spacetime curvature. Furthermore, we calculate the entanglement between mode pairs in all regimes of spacetime curvature. We obtain key, measurable signatures of horizon emission by the Hawking effect in an analogue system

Regimes of spacetime curvature.— The metric of spacetime in the vicinity of a Schwarzschild black hole can be expressed in the Painlevé-Gullstrand coordinates [47, 48]: in 1+1D its line element is $ds^2 = -(c^2 - \beta^2)dt^2 + d\zeta^2 + 2\beta dt d\zeta$, with the Newtonian escape velocity $\beta = (2Gm/\zeta_0)^{1/2}$, G the gravitational constant, m the mass of the black hole, ζ the spatial coordinate (ζ_0 is the spatial tortoise coordinate of the static observer [49–51]), t the proper time, and c the speed of light in vacuum. In this so-called “River Model” of the black hole, the metric describes ordinary flat space (and curved time), with space itself flowing towards $\zeta = 0$ (the spacetime singularity) at increasing velocity β [52, 53]. This acceleration of the flow velocity of space towards $\zeta = 0$ is the manifestation of the curvature of spacetime around the black hole: before the horizon, the flow velocity is subluminal, $\beta = c$ at the horizon (when $\zeta_0 = \zeta_{Schw}$, the Schwarzschild radius) and the flow

velocity of space is superluminal inside the horizon. The kinematics of waves propagating on this spacetime is determined by the curvature: for $\zeta_0 > \zeta_{Schw}$, motion is possible towards and away from the horizon, whereas for $\zeta_0 < \zeta_{Schw}$, motion is restricted from the horizon towards the singularity. Note that, upon a mere time-reversal of the metric, we obtain another regime of spacetime curvature — the white hole. Here, the kinematics of waves are such that motion in the interior region may only be directed from the singularity towards the horizon, whereas bi-directional motion is again possible in the outside region. That is, the white hole horizon prevents waves from entering the inside region.

Via the River Model, we understand the event horizon of the black (or white) hole as the interface between regions of sub- and superluminal space flow. In our optical analogue, such an interface is created by a step change in the refractive index of the medium in which light propagates. This RIF is illustrated in Figure 1 **a** in co-moving frame coordinates x and t .

The RIF separates two regions of homogeneous refractive index whose dispersion is modelled by [1]

$$c^2 k^2 = \omega^2 + \sum_{i=1}^3 \frac{4\pi\kappa_i\gamma^2(\omega + uk)^2}{1 - \frac{\gamma^2(\omega + uk)^2}{\Omega_i^2}}, \quad (1)$$

with ω and k the frequency and wavenumber in the frame co-moving with the RIF at speed u ($\gamma = [1 - u^2/c^2]^{-1/2}$). Ω_i and κ_i are the medium resonant frequencies and elastic constants. The change in index, δn , at $x = 0$ between the two regions is modelled by a change in κ_i and Ω_i in (1). As illustrated in Fig.1, δn manifests itself by a change in the dispersion relation between the low ($x > 0$, black curve) and high ($x < 0$, orange curve) refractive index regions. For a single frequency ω , the eight solutions of the polynomial (1) define eight discrete wavenumbers k : the eight ‘modes’ of the field. The Klein-Gordon norm of a mode is a constant of the motion, and is positive (negative) if the laboratory frame frequency $\Omega = \gamma(\omega + uk)$ is positive (negative) [1, 54]. Here, we focus on the optical frequency modes only. The detailed treatment [1] accounts for modes of all laboratory frame frequencies.

The dispersion curves in Fig.1 have the negative- (positive-) norm modes on the left (right). For all ω , there is one negative-norm mode and either three positive norm modes, or one positive norm mode [55]. One of the three positive-norm modes is the only mode solution of (1) with positive group velocity $\frac{\partial\omega}{\partial k}$. We call it ‘mid-optical’ — ‘*moL*’ on the left, and ‘*moR*’ on the right. There are also the ‘low optical’ mode *lo*, the ‘upper optical’ mode *uo*, and the ‘negative optical’ mode *no*. *lo*, *uo* and *no* all have negative group velocity. Thus at a frequency ω with three positive norm modes (k ’s), light may propagate in two directions: towards and away from the interface at $x = 0$. These kinematics are characteristic of a spacetime curvature with a subluminal space flow. We refer to these intervals as *subluminal intervals* (SbLIs): $[\omega_{minL}, \omega_{maxL}]$ and $[\omega_{minR}, \omega_{maxR}]$. Motion is restricted to the negative x dir-

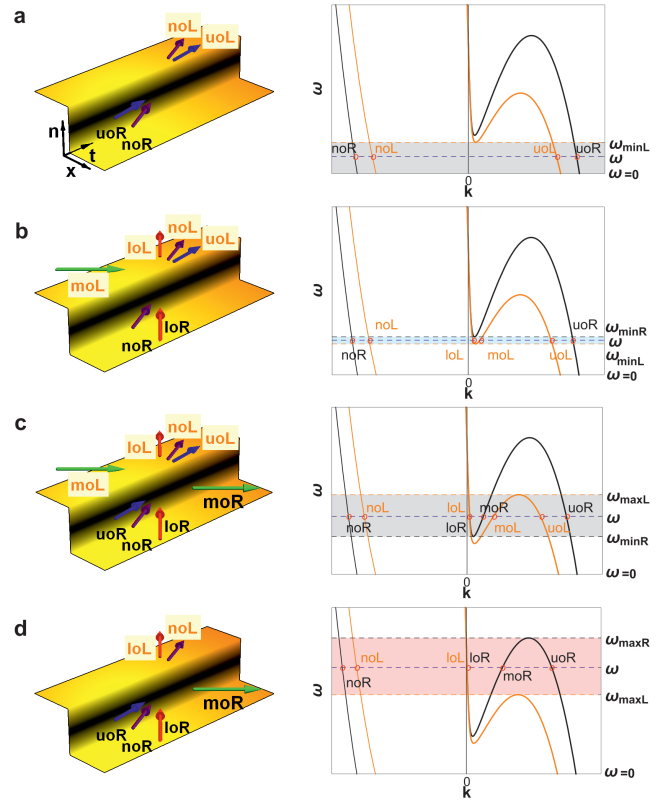


Figure 1. Possible kinematic configurations at the RIF. Time (left) and frequency (right) illustrations of propagating modes are shown for different comoving frequencies ω (**a-d**). The black (orange) dispersion curve corresponds to the low (high) index region. Single-frequency modes of ω are identified by intersections with the blue dashed line. Possible kinematic configurations, analogous to changes of spacetime curvature: **a**, horizonless configuration ($\omega < \omega_{minL}$); **b**, white hole configuration ($\omega_{minL} < \omega < \omega_{minR}$); **c**, horizonless configuration ($\omega_{minR} < \omega < \omega_{maxL}$); **d**, black hole configuration ($\omega_{maxL} < \omega < \omega_{maxR}$).

ection in all other frequency intervals, which we call *superluminal intervals* (SpLIs). Only in configurations **b** and **d** is a subluminal region paired with a superluminal region, creating a horizon — a white hole in **b** and a black hole in **d**. This is in analogy to the superluminal space flow in the interior region of a black- or white hole and the subluminal flow outside. *E.g.* in Figure 1 **d** a positive norm mode (*moR*) — Hawking radiation — allows for energy to propagate away from the hole in the subluminal region, while its negative norm partner (*noL*) falls inside the horizon.

This analysis shows that optical analogues give access to effects of gravity physics other than wave motion at the event horizon of black holes. For example, the kinematics over the horizonless frequency interval (Fig.1 **c**) are analogous to the change of curvature of spacetime induced by an incoming gravitational wave. Furthermore, considering all the four kinematic configurations (Fig.1 **a-d**) in a single system enables access to distinct regimes with and without horizons, and a comparison of their emission.

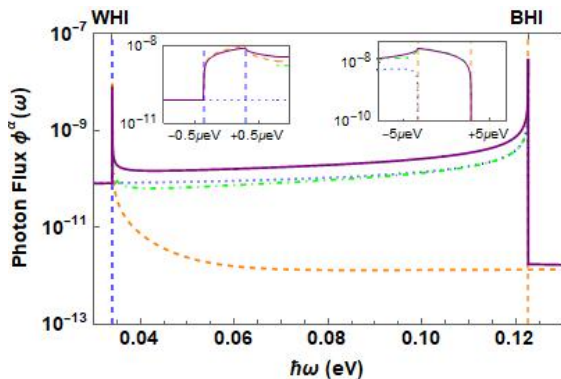


Figure 2. Spectra of photon flux (2) of the optical modes in the moving frame: *noL*, purple solid line; *uoL*, blue dotted line; *moR*, green dot-dashed line; *loL*, orange dashed line. Insets zoomed-in around the center frequency of the WHI and BHI.

We describe the transformation of ingoing modes into outgoing modes by the scattering matrix formalism and calculate the paired emission in all regimes of curvature. Our method to calculate the scattering matrix S_ω [1] allows us to analytically describe the mode coupling and takes all modes into account in all possible kinematic configurations for any RIF height, *i.e.*, refractive index change δn .

Quantum emission in all regimes of spacetime curvature.— We calculate spectra and mode-correlation maps to study the influence of the change in spacetime curvature on quantum emission. We present the properties of quantum emission as measured in the frame co-moving with the RIF, where the frequency (ω) is conserved. Note that the reference frames of optical and ‘fluid’ analogues [8, 11, 12, 14, 16, 17, 20–22] are exchanged: the rest frame of the moving fluid corresponds to the moving frame of the optical experiment, and vice versa. We emphasise that the spectra herein are directly comparable with those obtained for laboratory-frame observations in ‘fluid’ systems.

We compute the spontaneous photon flux in the moving frame [1]:

$$\phi^\alpha(\omega) = \frac{1}{2\pi} \sum_{\beta \notin \{\alpha\}} |S_{\alpha\beta}(\omega)|^2. \quad (2)$$

Here, $\{\alpha\}$ is the set of modes who have a positive (negative) norm if α is of positive (negative) norm. The photon flux results from the scattering of *in* modes into *out* modes of opposite norm. All *in* modes are in the vacuum state. In this paper, we consider the example of a RIF of height $\delta n = 2 \times 10^{-6}$, moving at $u = 2/3 c$ in bulk fused silica [1].

As can be seen in Fig.2, the spontaneous emission flux (2) peaks in two narrow frequency intervals. The low- and high-frequency intervals, white hole interval (WHI) and black hole interval (BHI), correspond to white and black hole emission, respectively. Over the horizon intervals (insets), the spectrum has a characteristic shark fin shape: on one side the overall emission cuts off by many orders of magnitude as the emit-

ting Hawking mode (*loL* or *moR*) ceases to exist. On the other side we enter kinematic scenario **c** (in Fig.1), leading to an abrupt decrease in emission. Outside these intervals, the emission decreases to a near constant level. All photons produced have partners of opposite norm and the emission follows the kinematics explored in Fig.1: for example, over the WHI, emission is mainly into modes *noL* (purple line) and *loL* (orange-dashed line). Over the BHI, emission is strongest into modes *noL* and *moR* (green-dot-dashed line). Because *noL* is the only negative norm mode of optical frequency, the flux in this mode is high.

The partnered emission can be characterised further by computing the matrix of photon number correlations between all modes. In what follows, we also plot the emission in non-optical modes. The photon-flux Pearson correlation coefficient between detectors 1 and 2 of bandwidth Δ_1 and Δ_2 , corresponding to modes α and α' , is [1]

$$C(\hat{N}_1^\alpha, \hat{N}_2^{\alpha'}) = \frac{\Delta^2}{\Delta_1 \Delta_2} \frac{\left| \sum_{\beta \notin \{\alpha\}} S_{\alpha\beta}^* S_{\alpha'\beta} \right|^2}{(\mathbf{v}^\alpha \mathbf{v}^{\alpha'})^{1/2}}, \quad (3)$$

with $\mathbf{v}^\alpha = 2\pi \phi^\alpha (2\pi \phi^\alpha + 1)$. Δ is the spectral overlap of detectors 1 and 2. \hat{N} is the photon number operator. The spectral correlation is an essential signature of the expected entanglement between photons of different wavelengths. Fig.3 shows correlations between all outgoing modes for typical frequencies ω and $\Delta_1 \Delta_2 = \Delta^2$. Correlations are generally strongest between the optical modes. Because *noL* is the unique negative-norm optical mode, we find strong correlations between this mode and positive-norm optical modes. The correlation coefficients are different if horizons exist (Fig.3 **b, d**). Over the WHI and BHI, there is only a single large correlation between *noL* and *loL*, and *noL* and *moR*, respectively. There, pairs of modes correspond to the Hawking emission mode and the partner in the WHI and the BHI. Without horizons (Fig.3 **a, c, e**), significant correlations exist between typically three mode pairs simultaneously.

To summarise, the flux of spontaneous emission is dominated by white- or black hole-horizon physics and drops significantly beyond that. Hence, the spectral characteristic is a ‘shark fin’ shape. Over the analogue white- and black hole intervals, paired two-mode emission at optical frequencies dominates

Horizon condition and entanglement.— Given the ample photon number correlations of Fig.3, we now proceed to assess the entanglement in the output state. Since the two-mode correlation coefficient does not reach unity at any frequency, photons in a positive norm mode will be paired with photons of different negative norm modes. As a result, the two-mode output will always be partially mixed.

Our measure of entanglement is the logarithmic negativity (LN) $E_{\mathcal{N}}$ [56, 57]. We calculate the LN between two output modes, tracing over the remaining state. In particular, we are interested in the only negative norm optical mode, *noL*, because all other optical modes are coupling mainly to

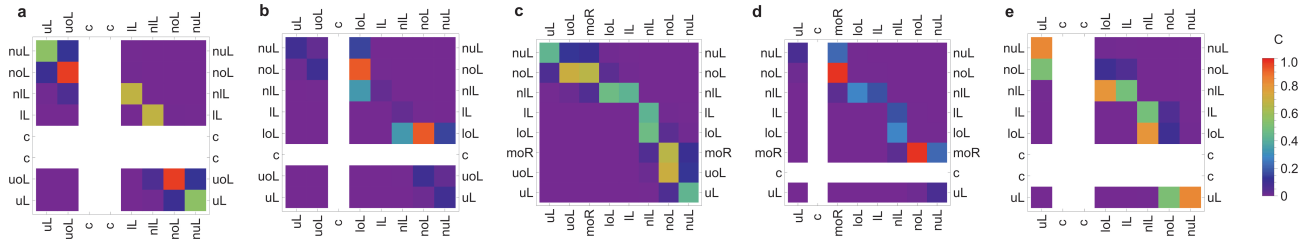


Figure 3. Photon number correlations between the 8 outgoing modes for five typifying frequencies: **a-d** as in Fig.1 and **e** for high ω ; c — a complex mode; ul , nl , ll , nul — non-optical modes.

this mode. In Fig. 4 the spectrum of the LN is shown for noL and each other positive norm mode. Similar to the emission spectra, the entanglement is peaked at both horizon intervals (WHI, BHI). Thus horizons efficiently entangle the light. However, E_N is an extensive quantity that increases with emission strength. In order to evaluate how strongly the photons of the two-mode state at the output are entangled, we compute the degree of entanglement \mathcal{J} . We define \mathcal{J} as the LN ($E_N^{\alpha_1\alpha_2}$) relative to the LN of a maximally entangled two-mode state of the same energy [58].

$$\mathcal{J} = \frac{E_N^{\alpha_1\alpha_2}}{4 \operatorname{arsinh} \left(\sqrt{\frac{\phi^{\alpha_1} + \phi^{\alpha_2}}{2}} \right)}, \quad (4)$$

In Fig.5, we plot the degree of entanglement for the same typifying frequencies as in Fig.3. The degree of entanglement is generally strongest between optical modes. In particular, the positive-norm optical modes moR and loL are close to being maximally entangled with mode noL over the black- and white-hole intervals, respectively (**b**, **d**). In other words, with horizons the Hawking mode and partner is in a close to maximally entangled, pure state. Without horizons (Fig.5 **a**, **c**, **d**), the degree of entanglement decreases for all mode pairs (except between modes uoL and noL in Fig.5 **a**) and the two modes are in a mixed state. Note that the degree of entanglement and the photon number correlations between modes

show a similar behaviour, although there is no direct mapping between them (see Appendix).

Conclusion.— We showed how strong dispersion can lead to novel multimode quantum dynamics stemming from the relation between horizon and horizonless emission in gravity analogues. Our work sheds light on the interplay between kinematics and parametric amplification in optics. The kinematic aspects of a physical system can thus be used to define quantum information processing tasks in a gravitational context.

We observed a striking transition in the quantum statistics when going from one kinematic scenario to the other, which we expect to be ubiquitous to gravity analogues, from optics through fluids to solid state. The influence of the kinematic scenario or regime of spacetime curvature is directly imprinted onto the quantum state. Hence we observed the entanglement and mixedness of any two-mode state to directly depend on it. These effects are largely robust against changes in dispersion and in the magnitude of the refractive index change [1, 58]. For our analysis we calculated the two-mode spectra as well as the logarithmic negativity of an optical analogue for the first time. This way we have put limits on the entanglement of an analogue system due to coupling to other modes than the Hawking pair. Particle number correlations and the degree of entanglement are key in characterising a variety of effects in all analogue gravity experiments such as cosmological pair creation by passing gravitational waves or expanding/contracting universes [20, 35, 59], the so-called black hole laser [60], analogue wormholes, and the quasi-bound states of black holes [61]. Importantly, the multimode analysis allows us to put limits on the thermality of the output state of spontaneous, quantum emission for the first time: since the degree of entanglement stays below unity, the state is not completely thermal (note that this is different from the considerations drawn in, *e.g.* [40, 41, 62] on the influence of the greybody factor on the thermal shape of the spectrum).

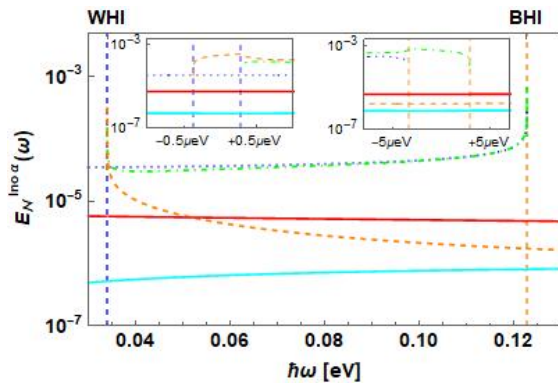


Figure 4. Entanglement of noL with the positive norm modes. ll , turquoise solid line; loL , orange dashed line; moR , green dot-dashed line; uoL , blue dotted line; uL , red solid line. Insets zoomed-in around the center frequency of the WHI and BHI.

ACKNOWLEDGEMENTS

The authors are thankful to Bill Unruh, Matthew Thornton, Viktor Nordgren and Valeria Saggio for insightful conversations. This work was funded by the EPSRC via Grant No. EP/L505079/1 and the IMPP.

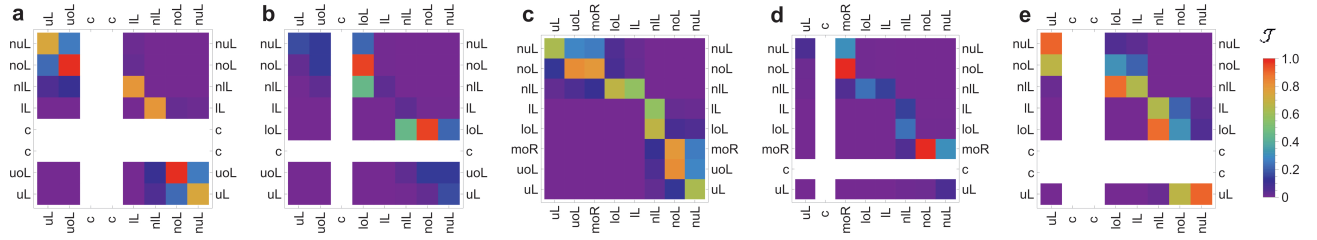


Figure 5. Degree of entanglement (\mathcal{E}) between the 8 outgoing modes for the five typifying frequencies of Fig.3. Here c indicates a complex mode; ul , nl , ll , nuL are the non-optical modes.

* maxime.jacquet@univie.ac.at

† fewk@st-andrews.ac.uk

- [1] Note1, jacquet M, Koenig F. Joint paper. To be published.
- [2] S. W. Hawking, *Nature* **248**, 30 (1974).
- [3] S. W. Hawking, *Communications In Mathematical Physics* **43**, 199 (1975).
- [4] W. G. Unruh, *Physical Review Letters* **46**, 1351 (1981).
- [5] T. G. Philbin, C. Kuklewicz, S. Robertson, S. Hill, F. König, and U. Leonhardt, *Science* **319**, 1367 (2008).
- [6] O. Lahav, A. Itah, A. Blumkin, C. Gordon, S. Rinott, A. Zayats, and J. Steinhauer, *Physical Review Letters* **105**, 240401 (2010).
- [7] A. Choudhary and F. König, *Optics Express* **20**, 5538 (2012).
- [8] J. Steinhauer, *Nature Physics* **12**, 959 (2016).
- [9] L.-P. Euvé, S. Robertson, N. James, A. Fabbri, and G. Rousseaux, arXiv:1806.05539 [gr-qc, physics:physics] (2018).
- [10] M. J. Jacquet, *Negative Frequency at the Horizon: Theoretical Study and Experimental Realisation of Analogue Gravity Physics in Dispersive Optical Media*, Springer Theses (Springer International Publishing, Vienna, 2018), ISBN 978-3-319-91070-3.
- [11] J. R. Muñoz de Nova, K. Golubkov, V. I. Kolobov, and J. Steinhauer, *Nature* **569**, 688 (2019).
- [12] G. Rousseaux, C. Mathis, P. Massa, T. G. Philbin, and U. Leonhardt, *New Journal of Physics* **10**, 053015 (2008).
- [13] D. Faccio, S. Cacciatori, V. Gorini, V. G. Sala, A. Averchi, A. Lotti, M. Kolesik, and J. V. Moloney, *Europhysics Letters* **89**, 34004 (2010).
- [14] S. Weinfurter, E. W. Tedford, M. C. J. Penrice, W. G. Unruh, and G. A. Lawrence, *Physical Review Letters* **106**, 021302 (2011).
- [15] H. Nguyen, D. Gerace, I. Carusotto, D. Sanvitto, E. Galopin, A. Lemaître, I. Sagnes, J. Bloch, and A. Amo, *Physical Review Letters* **114**, 036402 (2015).
- [16] L.-P. Euvé, F. Michel, R. Parentani, T. G. Philbin, and G. Rousseaux, *Physical Review Letters* **117**, 121301 (2016).
- [17] T. Torres, S. Patrick, A. Coutant, M. Richartz, E. W. Tedford, and S. Weinfurter, *Nature Physics* **13**, 833 (2017).
- [18] T. Torres, S. Patrick, M. Richartz, and S. Weinfurter, arXiv:1811.07858 (2018).
- [19] A. Posazhennikova, M. Trujillo-Martinez, and J. Kroha, *Phys. Rev. Lett.* **116**, 225304 (2016).
- [20] S. Eckel, A. Kumar, T. Jacobson, I. Spielman, and G. Campbell, *Physical Review X* **8** (2018).
- [21] J. Steinhauer, *Nature Physics* **10**, 864 (2014).
- [22] L.-P. Euvé and G. Rousseaux, *Physical Review D* **96**, 064042 (2017).
- [23] W. G. Unruh, *Foundations of Physics* **44**, 532 (2014).
- [24] A. Coutant and S. Weinfurter, *Physical Review D* **94**, 064026 (2016).
- [25] M. Tettamanti, S. L. Cacciatori, A. Parola, and I. Carusotto, *Europhysics Letters* **114**, 60011 (2016).
- [26] A. Parola, M. Tettamanti, and S. L. Cacciatori, *EPL (Europhysics Letters)* **119**, 50002 (2017).
- [27] A. Finke, P. Jain, and S. Weinfurter, *New Journal of Physics* **18**, 113017 (2016).
- [28] Y.-H. Wang, T. Jacobson, M. Edwards, and C. W. Clark, *Physical Review A* **96**, 023616 (2017).
- [29] Y.-H. Wang, M. Edwards, C. Clark, and T. Jacobson, *SciPost Physics* **3**, 022 (2017).
- [30] L. Parker, *Phys. Rev. Lett.* **21**, 562 (1968).
- [31] S. A. Fulling, *Phys. Rev. D* **7**, 2850 (1973).
- [32] R. Schützhold and W. G. Unruh, *Physical Review Letters* **107**, 149401 (2011).
- [33] A. Finke, P. Jain, and S. Weinfurter, *New Journal of Physics* **18**, 113017 (2016).
- [34] A. Fabbri and N. Pavloff, *SciPost Physics* **4** (2018).
- [35] D. Campo and R. Parentani, *Physical Review D* **74**, 025001 (2006).
- [36] X. Busch and R. Parentani, *Phys. Rev. D* **89**, 105024 (2014).
- [37] X. Busch, I. Carusotto, and R. Parentani, *Phys. Rev. A* **89**, 043819 (2014).
- [38] S. Finazzi and I. Carusotto, *Physical Review A* **90**, 033607 (2014).
- [39] D. Boiron, A. Fabbri, P.-E. Larré, N. Pavloff, C. I. Westbrook, and P. Ziñ, *Physical Review Letters* **115**, 025301 (2015).
- [40] A. Coutant and S. Weinfurter, *Physical Review D* **97**, 025006 (2018).
- [41] A. Coutant and S. Weinfurter, *Physical Review D* **97**, 025005 (2018).
- [42] A. V. Gorbach and D. V. Skryabin, *Nature Photonics* **1**, 653 (2007).
- [43] S. Hill, C. E. Kuklewicz, U. Leonhardt, and F. König, *Optics Express* **17**, 13588 (2009).
- [44] M. Jacquet and F. König, *Physical Review A* **92**, 023851 (2015).
- [45] M. Visser, *Classical and Quantum Gravity* **15**, 1767 (1998).
- [46] S. Finazzi and I. Carusotto, *Physical Review A* **87**, 023803 (2013).
- [47] P. Painlevé, *C. R. Acad. Sci (Paris)* **173**, 670 (1921).
- [48] A. Gullstrand, *Arkiv. Mat. Astron. Fys.* **16**, 1 (1922).
- [49] E. F. Taylor and J. A. Wheeler, *Exploring black holes: introduction to general relativity* (Addison Wesley Longman, San Francisco, 2000), ISBN 978-0-201-38423-9.
- [50] A. S. Eddington, *Nature* **113**, 192 (1924).
- [51] D. Finkelstein, *Physical Review* **110**, 965 (1958).
- [52] A. J. S. Hamilton and J. P. Lisle, *American Journal of Physics*

- 76, 519 (2008).
- [53] S. Braeck and Ø. Grøn, *Eur. Phys. J. Plus* **128:24** (2013).
- [54] E. Rubino, J. McLenaghan, S. C. Kehr, F. Belgiorno, D. Townsend, S. Rohr, C. E. Kuklewicz, U. Leonhardt, F. König, and D. Faccio, *Physical Review Letters* **108**, 253901 (2012).
- [55] Note2, at frequencies with only one positive norm mode, the two other mode solutions of Eq.(1) have become complex.
- [56] G. Vidal and R. F. Werner, *Physical Review A* **65**, 032314 (2002).
- [57] C. Weedbrook, S. Pirandola, R. Garca-Patrñ, N. J. Cerf, T. C. Ralph, J. H. Shapiro, and S. Lloyd, *Reviews of Modern Physics* **84**, 621 (2012).
- [58] Note3, Jacquet M, Koenig F. Further details on the calculation to be published elsewhere.
- [59] S. Weinfurter, P. Jain, M. Visser, and C. W. Gardiner, *Classical and Quantum Gravity* **26**, 065012 (2009).
- [60] J. L. Gaona-Reyes and D. Bermudez, *Annals of Physics* **380**, 41 (2017).
- [61] S. Patrick, A. Coutant, M. Richartz, and S. Weinfurter, *Physical Review Letters* **121**, 061101 (2018).
- [62] M. F. Linder, R. Schützhold, and W. G. Unruh, *Physical Review D* **93**, 104010 (2016).

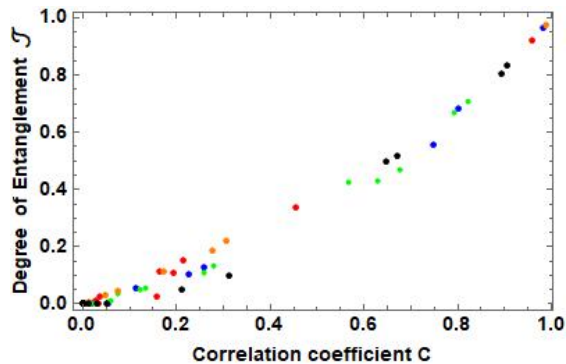


Figure 6. Relation between the degree of entanglement (4) and the photon-number correlations (3) for the 5 typifying frequencies of Fig.3 (a-e). Blue — low ω (cf. a); red — WHI (cf. b); green — medium ω (cf. c); orange — BHI (cf. d); black — high ω (cf. e).

Relation between the degree of entanglement and the photon-number correlations

The similarity of Figs.3 and 5 may suggest that the entanglement can be inferred from the photon-number correlations. Here we briefly explore this connection based on our numerical results.

In Fig.6, we plot the degree of two-mode entanglement \mathcal{J} against the corresponding correlation coefficient for each mode pair at each of the five typifying frequencies of Fig.3. We observe that \mathcal{J} is not a function of the correlation coefficient (3). In other words, there is no unique, one-to-one relation between the correlation coefficient and the degree of two-mode entanglement as measured via the logarithmic negativity. States of different degree of mixedness may exhibit the same correlation coefficient. Nevertheless, we remark firstly that even small correlation coefficients indicate entanglement and secondly that a correlation close to unity indicates close to maximal entanglement. It would be interesting to verify whether the non-uniqueness of the correspondence between the photon-number correlations and the degree of entanglement is specific to the measure of entanglement chosen — we leave these considerations to future investigations.